Tropical Cyclone Size Is Strongly Limited by the Rhines Scale: Experiments with a Barotropic Model

KUAN-YU LU[a] AND DANIEL R. CHAVAS[a]

[a] *Department of Earth, Atmospheric, and Planetary Sciences, Purdue University, West Lafayette, Indiana*

(Manuscript received 26 August 2021, in final form 22 March 2022)

ABSTRACT: Recent work found evidence using aquaplanet experiments that tropical cyclone (TC) size on Earth is limited by the Rhines scale, which depends on the planetary vorticity gradient β. This study aims to examine how the Rhines scale limits the size of an individual TC. The traditional Rhines scale is first reexpressed as a Rhines speed to characterize how the effect of β varies with radius in a vortex whose wind profile is known. The framework is used to define the vortex Rhines scale, which is the transition radius that divides the vortex into a vortex-dominant region at smaller radii, where the axisymmetric circulation is steady, and a wave-dominant region at larger radii, where the circulation stimulates planetary Rossby waves and dissipates. Experiments are performed using a simple barotropic model on a β plane initialized with a TC-like axisymmetric vortex defined using a recently developed theoretical TC wind profile model. The gradient β and initial vortex size are each systematically varied to investigate the detailed responses of the TC-like vortex to β. Results show that the vortex shrinks toward an equilibrium size that closely follows the vortex Rhines scale. A larger initial vortex relative to its vortex Rhines scale will shrink faster. The shrinking time scale is well described by the vortex Rhines time scale, which is defined as the overturning time scale of the circulation at the vortex Rhines scale and is shown to be directly related to the Rossby wave group velocity. The relationship between our idealized results and the real Earth is discussed. Results may generalize to other eddy circulations, such as the extratropical cyclone.

SIGNIFICANCE STATEMENT: Tropical cyclones vary in size significantly on Earth, but how large a tropical cyclone could potentially be is still not understood. The variation of the Coriolis parameter with latitude is known to limit the size of turbulent circulations, but its effect on tropical cyclones has not been studied. This study derives a new parameter related to this concept called the "vortex Rhines scale" and shows in a simple model how and why storms will tend to shrink toward this size. These results help explain why tropical cyclone size tends to increase slowly with latitude on Earth and can help us understand what sets the size of tropical cyclones on Earth in general.

KEYWORDS: Barotropic flows; Hurricanes/typhoons; Rossby waves; Tropical cyclones

1. Introduction

The size of a tropical cyclone (TC) determines its footprint of gale-force winds (Powell and Reinhold 2007), storm surge (Irish et al. 2011), and rainfall (Kidder et al. 2005; Lavender and McBride 2021). Therefore, understanding the dynamics of TC size is important for understanding potential TC impacts and risks.

Observational studies have found that TC size can vary significantly. For example, the TC radius of vanishing wind (R_0) typically ranges from 400 to 1100 km (Chavas et al. 2016). Past studies have shown that TC size may be sensitive to a variety of parameters, such as synoptic interaction (Merrill 1984; Chan and Chan 2013), time of the day (Dunion et al. 2014), environmental humidity (Hill and Lackmann 2009), intensity (Wu et al. 2015), and latitude (Weatherford and Gray 1988a,b; Chavas et al. 2016). On the f plane, TC size decreases with decreasing Coriolis parameter f following an f^{-1} scaling (Chavas and Emanuel 2014; Khairoutdinov and Emanuel 2013; Zhou et al. 2014), suggesting that size should decrease rapidly with latitude in the tropics. However, in observations, TCs size tends to increase slowly with latitude (Kossin et al. 2007; Knaff et al. 2014). Indeed, Chavas et al. (2016) showed explicitly that the inverse-f dependence cannot explain the observed dependence of TC size with latitude.

Recently, Chavas and Reed (2019, hereafter CR19) used aquaplanet experiments with uniform thermal forcing to demonstrate that median TC size scales with the Rhines scale (Rhines 1975). This scale depends inversely on the planetary vorticity gradient β and increases very slowly with latitude in the tropics, which matches the behavior seen in observations. Their findings lead to the following question: Is the size of an *individual* storm limited by the Rhines scale and, if so, why?

The Rhines scale has traditionally served as the scale that divides flow into turbulence and Rossby wave–dominated features (Held and Larichev 1996). When the eddy length scale is at or larger than the Rhines scale, the linear Rossby wave term dominates the nonlinear turbulent term. Conceptually, this implies that an eddy circulation larger than the Rhines scale behaves more wavelike. Despite being used to understand the role and scale of eddies in many large-scale atmospheric and oceanic circulation theories (e.g., James and Gray 1986; Vallis and Maltrud 1993; Held and Larichev 1996; Held 1999; Lapeyre and Held 2003; Schneider 2004; LaCasce and Pedlosky 2004), the Rhines scale has not been applied to understand the scale of the tropical cyclone. Since a TC can be

Corresponding author: Kuan-Yu Lu, lu711@purdue.edu

DOI: 10.1175/JAS-D-21-0224.1

regarded as an eddy circulation embedded in the tropical atmosphere, it seems plausible that the Rhines scale can indeed directly modulate TC size. Indeed, TCs are known to radiate Rossby waves in nature (Krouse et al. 2008; Schenkel and Hart 2015). However, it is not clear how β acts to limit the size of an individual TC and how this may be understood in the context of the Rhines scale.

The Rhines scale is typically calculated using a single characteristic turbulent velocity, usually defined as the root-mean-square velocity (e.g., Sukoriansky et al. 2006; Kidston et al. 2010), or a single characteristic velocity scale for a TC (an outer circulation velocity scale U_β in CR19; a collective velocity scale in Hsieh et al. 2020). However, a TC clearly does not possess a single velocity scale but instead has rotational velocities that vary strongly as a function of radius. Moreover, a theoretical model now exists for the radial structure of the TC wind field that captures the first-order behavior of TC structure found in observations (Chavas et al. 2015; Chavas and Lin 2016). Such a wind field model may be used to understand the detailed dynamics of this Rhines scale effect within a TC.

The simplest way to test the effect of β on a TC-like vortex is to perform two-dimensional nondivergent barotropic model simulations of a single TC-like vortex on a β plane, as the low-level circulation of a TC may be considered approximately barotropic (Sanders and Burpee 1968; DeMaria 1985; Chan and Williams 1987; Fiorino and Elsberry 1989) and the Rhines scale arises from the barotropic vorticity equation itself. As noted above, recent work has developed a model for the wind field in a hurricane that compares well with observations and so can be used to define a TC-like vortex as an initial condition. The use of a nondivergent barotropic model neglects the role of the secondary circulation, which is undoubtedly an important part of TC dynamics, in order to isolate the basic behavior and dynamical response of the primary circulation of a TC. Various aspects of the dynamics of a vortex on a β plane have been analyzed in past studies. The most widely known effect is β drift (Chan and Williams 1987), which is the poleward and westward vortex translation induced by the interaction of the vortex and the vortex-generated planetary Rossby waves[1] (Llewellyn Smith 1997; Sutyrin and Flierl 1994; Fiorino and Elsberry 1989; Wang et al. 1997). Notably, though not emphasized in their study, Chan and Williams (1987) demonstrated in their β-drift experiments that vortex size tends to decrease with time on a β plane. While inducing translation, these Rossby waves transfer kinetic energy from vortex to Rossby waves that then propagate into the environment (Flierl and Haines 1994; Sutyrin et al. 1994; Smith et al. 1995), thereby weakening the primary circulation and hence reducing vortex size (McDonald 1998; Lam and Dritschel 2001; Eames and Flór 2002). Eames and Flór (2002) found that for larger vortex size, the Rossby wave generation will dominate the dynamics of the vortex and, further, the vortex translation speed is correlated with the Rossby waves phase speed, a result that is conceptually similar to the Rhines scale effect described above. However, past work has yet to systematically test and explain the response of the size of an individual TC to β and place it in the context of the Rhines scale.

Here we focus on understanding the detailed response of the structure and size of an individual TC-like vortex to β. Our principal research questions are as follows:

1) How does the size of an individual TC-like vortex respond to β?
2) Can we develop a framework explaining why β limits storm size and its relationship to the traditional Rhines scale?
3) Can we predict the time-dependent response of TC size to β?

To answer these questions, we first revisit the meaning of the Rhines scale in the context of an individual coherent vortex and show how it may be reexpressed in the context of a vortex with a known wind profile to more transparently explain the response of an axisymmetric vortex to β. We then use this theory to analyze dynamical experiments using a simple barotropic model on a β plane initialized with the axisymmetric low-level tropical cyclone wind field defined in Chavas et al. (2015). This wind model can output a complete tropical cyclone radial profile of the tangential wind that mathematically merges two existing theoretical solutions (Emanuel 2004; Emanuel and Rotunno 2011), with a small number of physical parameters as input. We conduct experiments systematically varying β and initial vortex size to investigate the detailed time-dependent response of the vortex to β. Overall, our focus is on understanding the nature of the response of the size of a TC-like vortex to β and how we may use the conceptual foundation of the Rhines scale to predict it. Analysis of the details of energy transfer between the vortex and Rossby waves is left for future work.

The paper is organized as follows: section 2 presents the theory and proposes our hypotheses; section 3 demonstrates our model configuration and experimental design; section 4 presents the idealized results and analyses of our experiments; section 5 presents our key findings and discusses the implications of our results and their relationship to real TCs on Earth.

2. Theory

a. *The Rhines effect within a vortex*

The goal of this study is to investigate the limitation of vortex size by the Rhines scale, which is a parameter that governs the interaction between Rossby waves and a circulation in a fluid. This effect exists in any fluid in the presence of a planetary vorticity gradient $\beta = \partial f/\partial y$, where f is the Coriolis parameter and y is the meridional direction. The simplest such system is a dry barotropic (i.e., single-layer) fluid with constant

[1] We use the term "planetary" to emphasize that these Rossby waves arise due to vortex flow across the meridional vorticity gradient of Earth's rotation β. This is in contrast to "vortex Rossby waves" (Montgomery and Kallenbach 1997), which are Rossby waves that arise from vortex flow across the radial relative vorticity gradient of the vortex itself.

TABLE 1. Key variable names and definitions from the text.

Variable	Name	Definition
$U_c(r)$	Vortex circulation wind speed	Azimuthally averaged tangential wind speed of vortex circulation
Rh	Rhines number	Ratio between the nonlinear advection term and the β term
R_{Rh}	Rhines scale	The radius that a circulation with a given wind speed must have on a β plane to yield Rh = 1
U_{Rh}	Rhines speed	The tangential wind speed that a circulation at a given radius must have on a β plane to yield Rh = 1
R_{VRS}	Vortex Rhines scale	The radius within a vortex on a β plane where Rh = 1 ($U_{\mathrm{Rh}} = U_c$, $R_{\mathrm{Rh}} = r$)
U_{VRS}	Vortex Rhines speed	The tangential wind speed of the circulation at the R_{VRS}
T_{VRS}	Vortex Rhines time scale	The overturning time scale of the circulation at the R_{VRS}
R_2	2 m s^{-1} wind radius	The radius where the wind profile first reaches 2 m s^{-1} beyond the radius of maximum wind

depth. Such a fluid will obey the equation for conservation of absolute vorticity, which may be written as

$$\underbrace{\frac{\partial \zeta}{\partial t}}_{\text{Tendency term}} = \underbrace{-\mathbf{u}\cdot\nabla\zeta}_{\substack{\text{Nonlinear}\\ \text{advection term}}} \underbrace{-\beta v}_{\text{Beta term}}, \tag{1}$$

where $\partial/\partial t$ is the Eulerian tendency, ζ is the relative vorticity, $\mathbf{u}$ is horizontal wind velocity, v is the meridional wind speed, and β is the meridional gradient of planetary vorticity. The term on the left-hand side is the vorticity tendency, the first rhs term is the nonlinear advection of relative vorticity (hereafter "nonlinear term"), and the second rhs term is the linear advection of the planetary vorticity (hereafter "β term"). Note that, unlike a shallow-water system, this system has no gravity waves because the fluid depth is constant.

To determine which term in the barotropic vorticity equation dominates the vorticity tendency, a traditional scale analysis of Eq. (1) would yield

$$\frac{V}{LT} = -\frac{V^2}{L^2} - \beta V, \tag{2}$$

where the V is the speed scale of the wind, L is the horizontal length scale, and T is the time scale. For a nondivergent axisymmetric vortex, $\mathbf{u}$ and v can be both expressed as the azimuthal-mean tangential wind speed of the vortex circulation U_c. Note that U_c could be a function of radius if the structure of the vortex is known, as is done below. The advection term in Eq. (2) has L^2 in the denominator, but each L has a different physical meaning: the relative vorticity, $\zeta = (1/r)\partial(rU_c)/dr$, represents the radial gradient of U_c, and hence $L_\zeta = r$; in contrast, the advection operator, $\mathbf{u}\cdot\nabla$, is the tangential advection around the circumference of the vortex, and hence $L_{\mathbf{u}\cdot\nabla} = 2\pi r$. Together, in Eq. (2), the denominator becomes $L^2 = 2\pi r^2$. Therefore, the ratio between the nonlinear advection term and the β term, which we define as the Rhines number (Rh), can be written as following:

$$\frac{\mathbf{u}\cdot\nabla\zeta}{\beta v} \equiv \mathrm{Rh} \approx \frac{\frac{U_c^2}{2\pi r^2}}{\beta U_c} = \frac{U_c}{2\pi\beta r^2}. \tag{3}$$

Equation (3) neglects any mean radial flow as is required for a barotropic vortex. Real TCs possess significant inflow at low levels, which is a topic we address in the discussion of our results below.

When Rh = 1, the nonlinear term and the β term are equal (Vallis 2017, p. 446). We can rearrange Eq. (3) to define the Rhines scale (R_{Rh}) for a rotational flow with speed of U_c:

$$R_{\mathrm{Rh}} \equiv \sqrt{\frac{U_c}{2\pi\beta}}. \tag{4}$$

Note that the key distinction of Rhines scale from a deformation-type scale is that the velocity scale is a true flow speed rather than a gravity wave phase speed. We emphasize that we are precise in including the 2π factor in our explanation above, as it is quantitatively important for our results presented below. This is in contrast to typical scale analyses, which are agnostic to the inclusion or neglect of constant factors (and indeed the appearance of such factors varies in the literature).

Previous studies tend to estimate a system's Rhines scale by assuming a characteristic eddy flow velocity (e.g., CR19; Chemke and Kaspi 2015; Frierson et al. 2006), such that the system will have a single characteristic Rhines scale. However, an individual TC-like vortex possesses circulation speeds that vary strongly with radius and hence contains both "small" and "large" circulations simultaneously by definition. Thus, the details of these wave effects should depend on radius and cannot be characterized by a single velocity nor a single Rhines length scale. The simplest starting point is to consider the vortex as comprised of independent circulations at each radius with different wind speeds and calculate their corresponding Rhines scale as a function of radius. This results in a radial profile of R_{Rh} that depends on the vortex's tangential wind profile and β [Eq. (4)]. Here we use the wind speed of the TC's circulation (U_c), which varies with radius, to calculate the radial profile of the Rhines scale in a TC. This allows one to evaluate how β may affect the vortex circulation differently at different radii.

The Rhines scale (R_{Rh}) is defined as the radius that a given circulation speed would have to be at to yield Rh = 1 (see Table 1). For a sufficiently large circulation relative to the Rhines scale ($r \gg R_{\mathrm{Rh}}$), the nonlinear term is small (Rh $\ll$ 1) and thus its vorticity tendency will be governed by the β term, which gives pure Rossby waves. Therefore, a circulation at a

given radius that is larger than its corresponding Rhines scale will be affected by β and generate Rossby waves, which will radiate energy away. Meanwhile, for a sufficiently small circulation relative to the Rhines scale ($r \ll R_{\mathrm{Rh}}$), the β term is small (Rh $\gg$ 1), and thus its vorticity tendency will be governed by the nonlinear term and will generate minimal Rossby wave activity. For a perfectly axisymmetric vortex, the relative vorticity advection term is zero, and hence the circulation can remain quasi steady.

The concept of the Rhines scale for a vortex can be more easily understood if rephrased in terms of a velocity scale rather than length scale. Since R_{Rh} is function of U_c [Eq. (4)], that means for a given wind speed, R_{Rh} defines a specific length scale whose value relative to the circulation radius determines whether the circulation will generate significant Rossby waves or not. Alternatively, one may choose to fix the circulation radius, in which case Rh equivalently defines a specific wind speed whose value relative to the circulation wind speed determines whether the circulation will be affected by Rossby waves or not. Based on this concept, we can rearrange the Eq. (3) to yield the wind speed when Rh = 1, which we define as the Rhines speed (U_{Rh}):

$$U_{\mathrm{Rh}}(r) \equiv 2\pi\beta r^2. \tag{5}$$

We write the Rhines speed in this equation as $U_{\mathrm{Rh}}(r)$ to emphasize that this quantity varies with radius. Note that R_{Rh} [Eq. (4)] now will also be a function of radius because U_c is a function of radius. Importantly, while the radial dependence of R_{Rh} is a function of both β and U_c, the radial dependence of U_{Rh} is solely a function of β [Eq. (5)]. Hence, for a given value of β, the radial profile of U_{Rh} is fixed and is independent of the vortex. The case $U_c \ll U_{\mathrm{Rh}}$ is analogous to $r \gg R_{\mathrm{Rh}}$ and corresponds to the wave-dominant regime, while the case $U_c \gg U_{\mathrm{Rh}}$ is analogous to $r \ll R_{\mathrm{Rh}}$ and corresponds to the vortex-dominant regime. The above definition is especially convenient because the radial structure of the circulation may be known or specified.

Finally, if the radial profile of the vortex flow U_c is specified and decays monotonically with radius, then there will be a single radius where $U_c(r)$ and $U_{\mathrm{Rh}}(r)$ intersect. We define this radius as the vortex Rhines scale R_{VRS}, i.e.,

$$R_{\mathrm{VRS}} : U_c(r = R_{\mathrm{VRS}}) = U_{\mathrm{Rh}}(r = R_{\mathrm{VRS}}). \tag{6}$$

R_{VRS} corresponds to the radius within the vortex where Rh = 1, marking the transition between a vortex-dominant regime at smaller radii ($r < R_{\mathrm{VRS}}$, Rh > 1) and a wave-dominant regime at larger radii ($r > R_{\mathrm{VRS}}$, Rh < 1). We define the flow speed at R_{VRS} as the vortex Rhines speed U_{VRS}, i.e.,

$$U_{\mathrm{VRS}} = U_c(R_{\mathrm{VRS}}). \tag{7}$$

We may further define the turnover time scale of the circulation at R_{VRS} as the vortex Rhines time scale T_{VRS} given by

$$T_{\mathrm{VRS}} = \frac{2\pi R_{\mathrm{VRS}}}{U_{\mathrm{VRS}}}. \tag{8}$$

Note that T_{VRS} is also the dominant time scale associated with the R_{VRS} in a TC-like vortex; the physical interpretation of this time scale will be discussed in section 4d and 4g. We emphasize that R_{VRS}, U_{VRS}, and T_{VRS} are each a single value for the entire vortex and not a function of radius.

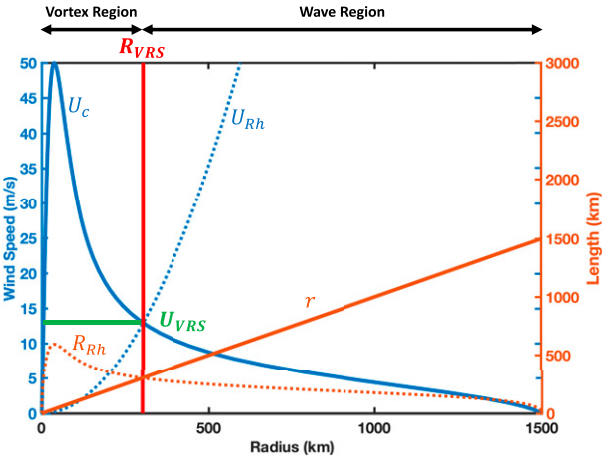

FIG 1. Conceptual diagram of the vortex Rhines scale (R_{VRS}, red vertical line) defined by the vortex's tangential wind profile (U_c, blue solid line) and the Rhines speed profile [U_{Rh}, Eq. (5), blue dashed line]. Brown dashed line represents the Rhines scale at each radius [R_{Rh}, Eq. (4)], and green horizontal line indicates the vortex Rhines speed (U_{VRS}). Regions with different dynamical features are labeled: inside R_{VRS} is the vortex region, and outside R_{VRS} is the wave region.

b. *Illustrative example*

To visualize the theory, Fig. 1 displays an example radial profile of U_c (blue solid line) for a tropical cyclone, defined by the model for the low-level tangential wind of Chavas et al. (2015; described in detail in section 3 below). The figure also displays the radial profiles of the Rhines speed U_{Rh} [Eq. (5); blue dashed line] and the traditional Rhines scale R_{Rh} [Eq. (4); brown dashed line]. Typically, a TC-like U_c profile will decrease monotonically with radius outside the radius of maximum wind. Meanwhile, the U_{Rh} (blue dashed line in Fig. 1) profile increases with radius monotonically. Therefore, there is an intersection between these two curves at a specific radius given by the vortex Rhines scale (R_{VRS}, red vertical line). The vortex Rhines speed U_{VRS} is also marked (green horizontal line).

Analogous to the traditional Rhines scale separating wave and vortex dominant regimes, R_{VRS} divides the vortex into a vortex-dominant region at smaller radii and a wave-dominant region at larger radii, as shown by Fig. 1. In the vortex region at smaller radii, planetary Rossby waves are not readily generated and the rapid rotation will axisymmetrize the vorticity field (Montgomery and Kallenbach 1997) until the vortex flow is parallel to the vorticity contours and the flow becomes quasi steady [Eq. (1)]. Meanwhile, in the wave region at larger radii, the rotating flow is slow enough to generate significant planetary Rossby wave activity, which will cause asymmetric deformation of the vortex flow at those radii.

Taken together, the expectation is that only the circulation in the wave-dominant region will stimulate significant planetary Rossby waves, distorting and gradually dissipating the circulation therein. Meanwhile, the circulation in the vortex-dominant region would be expected to remain nearly steady. As a result, vortex size will be limited by R_{VRS}. We emphasize again that these are planetary Rossby waves and not vortex Rossby waves generated by the vortex flow.

c. Hypotheses

To investigate how R_{VRS} affects the size of a TC-like vortex, we propose following hypotheses:

1) Vortex size is limited by its vortex Rhines scale, R_{VRS}.
2) A larger vortex relative to its vortex Rhines scale will shrink faster.

Below we test these hypotheses by simulating a TC-like vortex on a β plane. We focus here on characterizing and understanding the vortex response to β across experiments varying TC size and β. Theoretical analysis of the detailed energetics of this response is left to future work.

3. Methods

a. Barotropic model

This study uses a nondivergent, dry barotropic model to simulate the vortex behavior on a β plane. We use the open-source model developed by James Penn and Geoffrey K. Vallis (available at http://empslocal.ex.ac.uk/people/staff/gv219/codes/barovort.html). It uses a pseudospectral method with double-periodic boundary conditions to solve the barotropic vorticity equation [Eq. (1)] in 2D space. The model is set up with 500 grid points in both x and y directions, with grid spacing of 20–40 km depending on the experiment. The initial time step is 60 s and an adaptive time step is used thereafter to avoid violating the CFL condition. The forcing amplitude factor is set as zero. For numerical stability, the model applies a high wavenumber Smith filter (Smith et al. 2002) as the dissipation process, which damps any structure that has a wavenumber larger than 30. Experiments with different wavenumber threshold are tested (40, 50, and 60) and the results are not sensitive to this choice (not shown).

There are two principal advantages of using such a simple barotropic model. First, since the barotropic vorticity equation only includes relative and planetary vorticity advection terms, it is an ideal tool to isolate the dynamical details of the Rhines effect on a TC-like vortex. Second, the barotropic model is nondivergent and hence neglects the boundary layer inflow and upper level outflow found in a real TC. As a result, the barotropic model neglects azimuthal-mean radial mass transport while still permitting eddies to transport momentum radially. In doing so, the model can still simulate the vortex response to beta while minimizing interaction across radii within the vortex. This helps simplify understanding of the dynamical response of the vortex.

b. Tropical cyclone wind field model

Since our interest is in tropical cyclones, we employ the model of Chavas et al. (2015, hereafter C15 model) for the complete radial profile of the TC low-level tangential wind field to initialize the barotropic model. C15 model is a theoretical model that can reproduce the first-order structure of the TC wind field and also dominant modes of wind field variability (Chavas and Lin 2016). The model wind profile may be specified by a small number of storm and environmental physical parameters. The storm parameters are the maximum wind speed (V_{max}), the outer radius of vanishing wind (R_0), and the Coriolis parameter, f; the environmental parameters are the clear-sky free-tropospheric radiative-subsidence rate (w_{cool}), the surface drag coefficient (C_d) for the outer region, and the ratio of surface coefficients of enthalpy and drag (C_k/C_d). In this study, for the model code (Chavas 2022), we fix $w_{cool} = 0.002$ m s^{-1}, $C_d = 0.0015$, and $C_k/C_d = 1$, all held constant, and we apply no adjustment within the eye. We set the Coriolis parameter to be constant at its value at 10°N in order to keep our initial wind profile fixed with respect to f, including for our experiments varying β below. On the sphere this would not be possible since f and β both depend on latitude. Here though we seek to isolate the effect of varying β alone, which can conveniently be done in a β-plane model since f does not appear in the governing equation at all. Note that for the set of input parameters given above, the C15 model will implicitly predict the radius of maximum wind (R_{max}). To input the vortex into the barotropic model, the wind profile is transformed into an axisymmetric vorticity field and placed at the domain center to define the barotropic model's initial condition.

c. Experiments

The initial wind profiles for all experiment sets described below are listed in Table 2.

1) CONTROL EXPERIMENT

We define our Control experiment ("CTRL") as a simulation with a uniform quiescent environment and a single vortex at the domain center. β is fixed at a value of 2.2547×10^{-11} m^{-1} s^{-1} corresponding to a latitude of 10°N; on the rotating sphere $\beta = 2(\Omega/a)cos(\phi)$, where Ω is the planetary rotation rate, a is the planetary radius, and ϕ is latitude. The vortex has $V_{max} = 50$ m s^{-1} and $R_0 = 1500$ km. The CTRL is used below to illustrate the basic vortex response on a low latitude β plane.

In our experiment framework, when inserting a TC-like vortex into the f plane (setting $\beta = 0$), the tangential wind profile will exhibit an initial adjustment at small radii but then will remain very steady for many tens of days as shown in Fig. 2. Despite the initial inner-core structural adjustment, the outer circulation remains nearly unchanged from its initial state. This result demonstrates that the vortex circulation is spun up and the vortex responses presented below are due solely to the imposition of β. Thus, in all experiments we first simulate a 5-day spinup period with $\beta = 0$, after which β is instantaneously turned on to a constant value for the subsequent 95 days or shorter if the vortex has reached quasi

TABLE 2. Parameter values for experiments in each experiment set described in the text.

	R_0 (km)	β	V_{max} (m s^{-1})	Grid space (km)
VARYR0	600	10°N	50	20
	700	10°N	50	20
	800	10°N	50	20
	900	10°N	50	20
	1000	10°N	50	30
	1100	10°N	50	30
	1200	10°N	50	40
	1500	10°N	50	40
	1800	10°N	50	40
VARYBETA	1500	10°N	50	40
	1500	20°N	50	40
	1500	30°N	50	40
	1500	40°N	50	40
	1500	50°N	50	40
	1500	60°N	50	40
	1500	70°N	50	40
	1500	80°N	50	40
VARYVMAX	1500	10°N	20	40
	1500	10°N	30	40
	1500	10°N	40	40
	1500	10°N	50	40

equilibrium. Finally, since a vortex on a β plane will gradually drift with time, we define the centroid of the vorticity to track the vortex center with time and use this to calculate a storm-centered radial profile of the tangential wind at each time step.

2) EXPERIMENT SET "VARYVMAX": VARYING VORTEX INITIAL INTENSITY

In our experiments, resolution limitations will cause vortices with different initial sizes to have different initial intensities because the inner core is poorly resolved; this effect acts similar to a radial mixing and hence acts to decrease V_{max} and increase R_{max}. Thus, we design experiment set "VARYVMAX" (Fig. 3a), which has vortices with different initial intensities at fixed size to examine the impact of vortex intensity on the evolution of the vortex circulation. Note that the outer tangential wind structure remains constant as intensity is varied, which is by design in the C15 model as the inner and outer circulations of TCs tend to vary independently.

3) EXPERIMENT "VARYR0": VARYING VORTEX INITIAL SIZE

To investigate the effect of the Rhines scale on vortices with different sizes, we design experiment set "VARYR0" (Fig. 3b), which has initial wind profiles specified using R_0 over a range of values from 600 to 1800 km (see Table 2) with β fixed at the *CTRL* value. Since all the members in this experiment set have the same value of β, they all have the same U_{Rh} profile. Thus, when increasing R_0, the vortex wind profile expands outward, and as a result, R_{VRS} increases as R_0 increases.

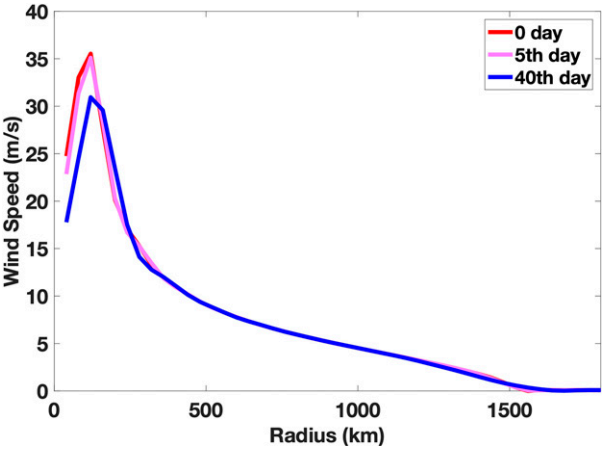

FIG 2. Evolution of the CTRL azimuthal-mean tangential wind profile (solid lines in different colors) on the f plane (β= 0) at days 0, 5, and 40.

4) EXPERIMENT SET VARYBETA: VARYING β

To investigate the effect of the Rhines scale on vortex size at different values of β, we design experiment set "VARYBETA" (Fig. 3c), which imposes the CTRL wind profile for all members on a β plane with β over a range of values from 2.2547×10^{-11} to 3.9756×10^{-12} m^{-1} s^{-1}, corresponding to a latitude of 10° to 80°N on Earth (recall that β decreases moving poleward). As noted above, f in the C15 model is held constant at its CTRL value to isolate effects of β on vortex evolution at fixed initial vortex structure. The Rhines speed increases at all radii with increasing β [Eq. (5)], and as a result R_{VRS} decreases as β increases.

4. Results

a. *Vortex response: CTRL*

We begin by describing the simulated response of our Control vortex to β and place it in the context of the vortex Rhines scale. Figure 4 shows the structural evolution of CTRL. Figure 4a shows the time series of the radius of 2 m s^{-1} wind (hereafter R_2) of this vortex, which we use as our measure of the overall size of the storm, as well as the value of the Rhines scale evaluated at 2 m s^{-1} given by $R_{2Rh} = R_{Rh}$ (U_c = 2 m s^{-1}) [Eq. (4)], and the initial vortex Rhines scale (R_{VRS_0}) of this vortex; It took approximately 20 days for R_2 to shrink to a quasi-equilibrium value that is slightly smaller than R_{VRS_0}. Note that R_2 is reduced by half after only 5 days, and the equilibrium value of R_2 is still larger than R_{2Rh}. However, the relationship between final equilibrium size and the Rhines scale magnitude depends strongly on the choice of wind speed used to define size; in the limit of U_c = 0 m s^{-1}, the Rhines scale is zero. This demonstrates a shortcoming of the traditional Rhines scale for defining a precise limit on vortex size, which motivates the use of the vortex Rhines scale, which does not require choosing an arbitrary wind speed, in our subsequent analyses.

Figure 4b demonstrates the structural evolution of CTRL. The outer circulation is largely dissipated within 40 days, yielding a profile that decreases rapidly to zero. Note that, aside from

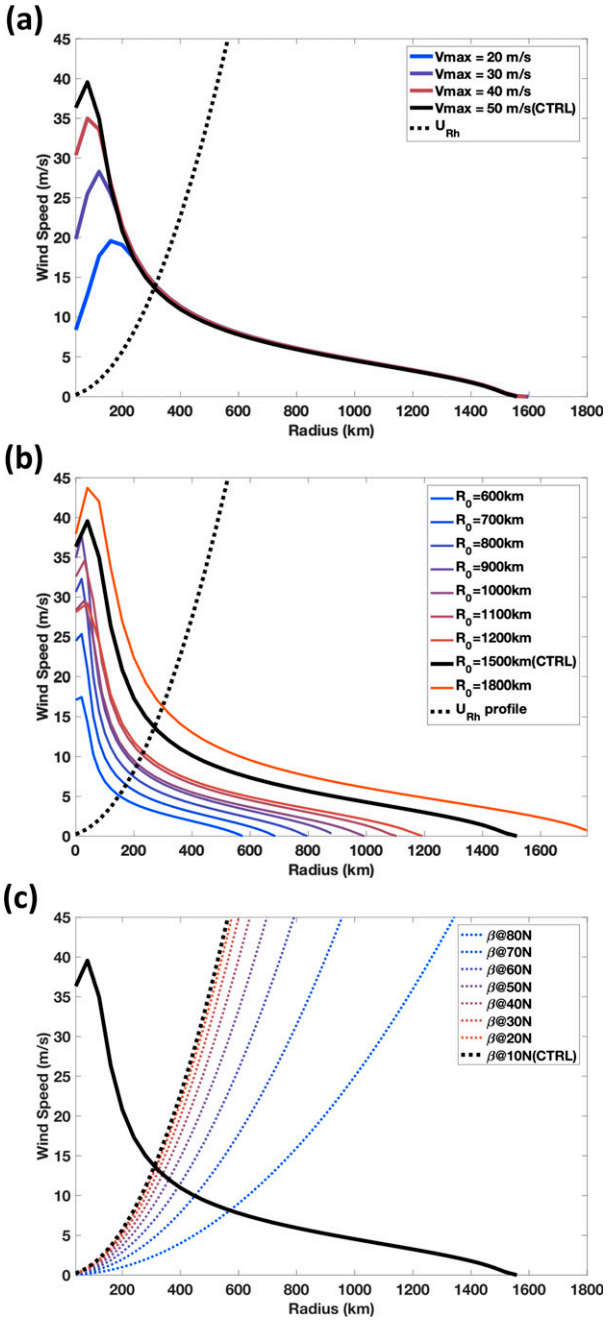

FIG 3. Initial azimuthal-mean tangential wind profiles (U_c, solid) and Rhines speed profiles (U_{Rh}, dashed) for all experiments within each of our three experiment sets. (a) VARYVMAX, varying initial V_{max}, with U_{Rh} profile in dashed black. (b) VARYR0, varying initial outer size. (c) VARYBETA, varying β, with U_{Rh} profiles in colored dashed lines. The CTRL profile is represented by the black solid curve across all plots.

a very slow decrease in V_{max}, the inner-core structure remains nearly steady and does not feel the large change in the outer circulation. This behavior would not be expected for a real TC as the radial inflow would communicate the response of the outer circulation inwards to smaller radii. Our nondivergent barotropic model does not permit mean inflow, though. Thus, the radial structure of the vortex in our model is free to evolve away from the realistic structure imposed in the initial condition. As a result, the final vortex structure found here is purely the outcome if β alone is allowed to act on a vortex.

Figures 4c–e display a detailed 2D analysis of the vortex at different stages of its evolution based on Fig. 4a: the initial state (day 0), the shrinking stage (day 5), and the quasi-equilibrium stage (day 40). Figure 4b shows the azimuthal-mean tangential wind profile at each stage. To demonstrate the dominant term in Eq. (1), we calculate the base-10 logarithm of the Rhines number, $\log_{10}$Rh, at each grid point (a value of zero corresponds to Rh = 1). Figures 4c–e show storm-centered maps of absolute wind speed and $\log_{10}$Rh at each stage, with warmer colors (positive $\log_{10}$Rh) representing the vortex-dominant regime and cooler colors (negative $\log_{10}$Rh) representing the wave-dominant regime and with R_{VRS} shown as a red circle. Initially, the vortex R_2 is larger than the R_{VRS} but no asymmetric structure has yet developed within the vortex. During the shrinking stage, the vortex size decreases rapidly, as the outer circulation outside of R_{VRS} is highly variable and azimuthally asymmetric compared to the inner core circulation inside of R_{VRS}. At small radii, the nonlinear term is generally dominant, which is evidenced by the warmer colors (positive $\log_{10}$Rh); at larger radii the wave term is generally dominant, which is evidenced by the colder colors (negative $\log_{10}$Rh). Note that R_{VRS} approximately separates the two regions. Finally, in the quasi-equilibrium stage, the circulation has nearly vanished in the wave region outside of R_{VRS} while it remains intact and highly axisymmetrized inside of R_{VRS}.

CTRL demonstrates how the radial structure of the response of a single vortex on a β plane can be described at least qualitatively via R_{VRS}. The vortex Rhines scale appears to impose a strong limit on vortex size by dividing the vortex into two regions with distinct dynamical characteristics. Circulations in the vortex region produce minimal Rossby waves and instead are simply self-advected, thus maintaining a highly axisymmetric structure. In contrast, circulations in the wave region generate significant Rossby wave activity that produce a highly azimuthally asymmetric structure that acts to spin down the circulation there.

b. *Response with varying V_{max}*

Since we have intensity variability within our experiment members due to resolution limitations, it is important to demonstrate that changes in inner core intensity do not affect the outer circulation before we analyze any experiments systematically. Figure 5a shows the R_2 time series of all members in VARYVMAX. All members exhibit a nearly identical size evolution across experiments. These results indicate that variations in intensity changes the wind speeds in the vortex region ($r \ll R_{VRS}$) but not the broad outer circulation. This result suggests that the vortex size evolution is not sensitive to the decrease in intensity due to the coarse horizontal resolution. An experiment identical to CTRL but at finer horizontal

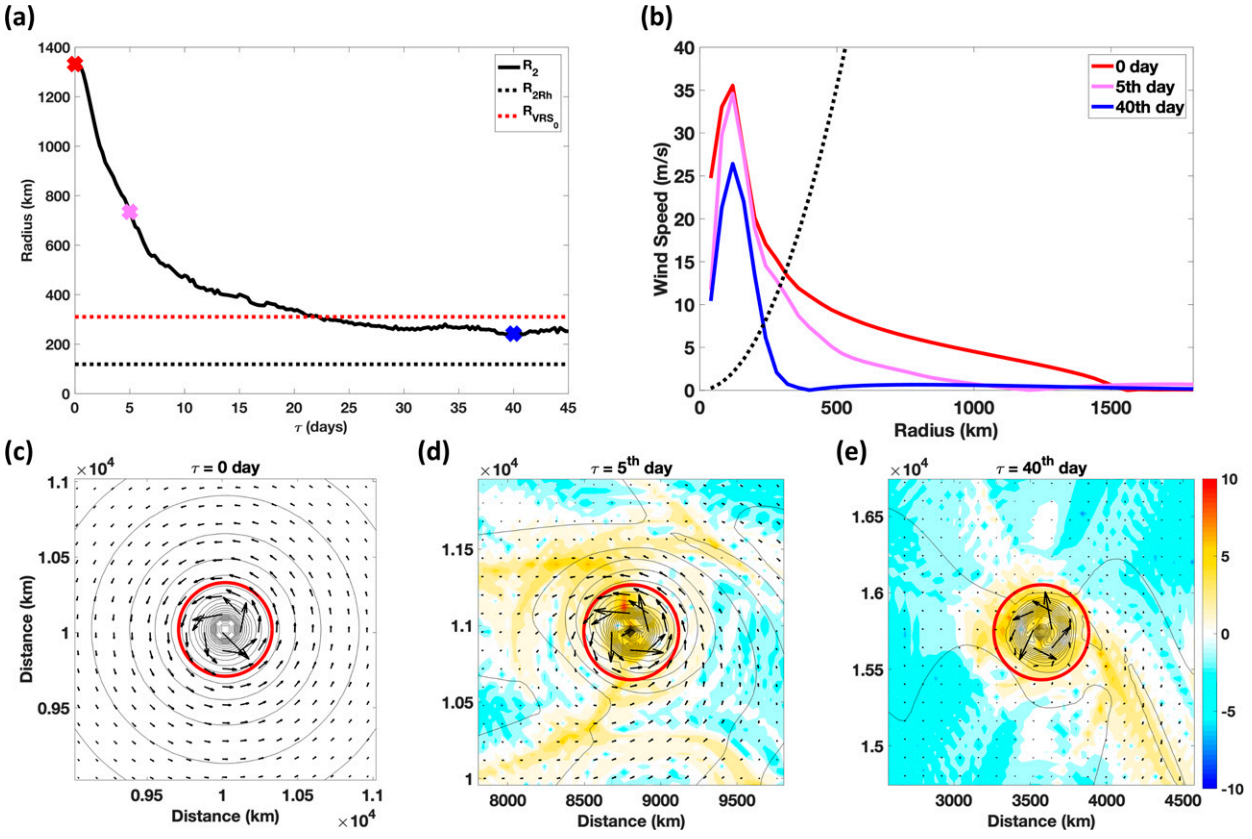

FIG 4. Results of CTRL. (a) R_2 (radius of 2 m s^{-1}) time series, where τ indicates time since β is turned on; markers indicate times from the initial stage (day 0, red cross), the shrinking stage (day 5, pink cross), and the quasi-equilibrium stage (day 40, blue cross), the black dashed line represents the Rhines scale of 2 m s^{-1} wind [$R_{2\mathrm{Rh}}$, Eq. (4)], and the red dashed line represents the initial R_{VRS}. (b) U_c profiles at each of the three stages and U_{Rh} profile (black dashed curve). (c)–(e) Wind speed (black contours), wind vector (black arrows), $\log_{10}$Rh (shading), and R_{VRS} (red circle) at each of the three stages, respectively.

resolution yields very similar results (not shown). Note that in a barotropic model there is no secondary circulation that links the intensity change in inner core to the distant outer circulation, as there would be in a real TC. However, the low-level circulation of a TC is characterized by inflow at nearly all radii and so the outer circulation would not be expected to directly feel changes in inner-core structure, a behavior also common to observed and simulated TCs (Frank 1977; Merrill 1984; Chavas and Lin 2016; Rotunno and Bryan 2012).

c. *Responses with varying initial R_0 or β*

Figure 5b shows the R_2 time series of all members in *VARYR*0. Warmer colors indicate members with larger initial vortex size. In VARYR0, vortices with larger initial size shrink faster, but they all gradually converge in size and eventually reach a quasi equilibrium of approximately 200–300 km.

Figure 5c shows the R_2 time series of all members in VARYBETA. Warmer colors indicate members with larger β (lower Earth latitude). Each vortex in VARYBETA has the same U_c profile and hence all time series start from the same R_2 value. In VARYBETA, experiments at larger β (lower latitude) will shrink in size faster. The results of VARYBETA demonstrate how the vortex Rhines effect becomes weaker at higher latitude, where β is smaller. For smaller β, R_{VRS_0} is larger, yielding a slower size shrinking rate and larger quasi-equilibrium size. The result that storm size increases with latitude consistent with the Rhines scale was also found in aquaplanet experiments in CR19.

The R_2 time series analysis demonstrates the systematic behavior and their differences between VARYR0 and VARYBETA. First, all members in both experiments shrink in size at different rates after β is turned on. Second, vortex size shrinks at a faster rate for larger initial R_0 at fixed β or for larger β at fixed initial R_0. This similarity arises because all members from each experiment have different initial sizes relative to their vortex Rhines scale. Therefore we next examine the size evolution of each member in a nondimensional sense relative to their R_{VRS} to provide more general physical insight into the results of these experiments.

d. *Vortex size evolution: Nondimensional space*

To generalize the vortex size evolution across VARYR0 and VARYBETA, we next examine the evolution of R_2 nondimensionalized by the initial R_{VRS} (R_{VRS_0}), R_2/R_{VRS_0}, for each member.

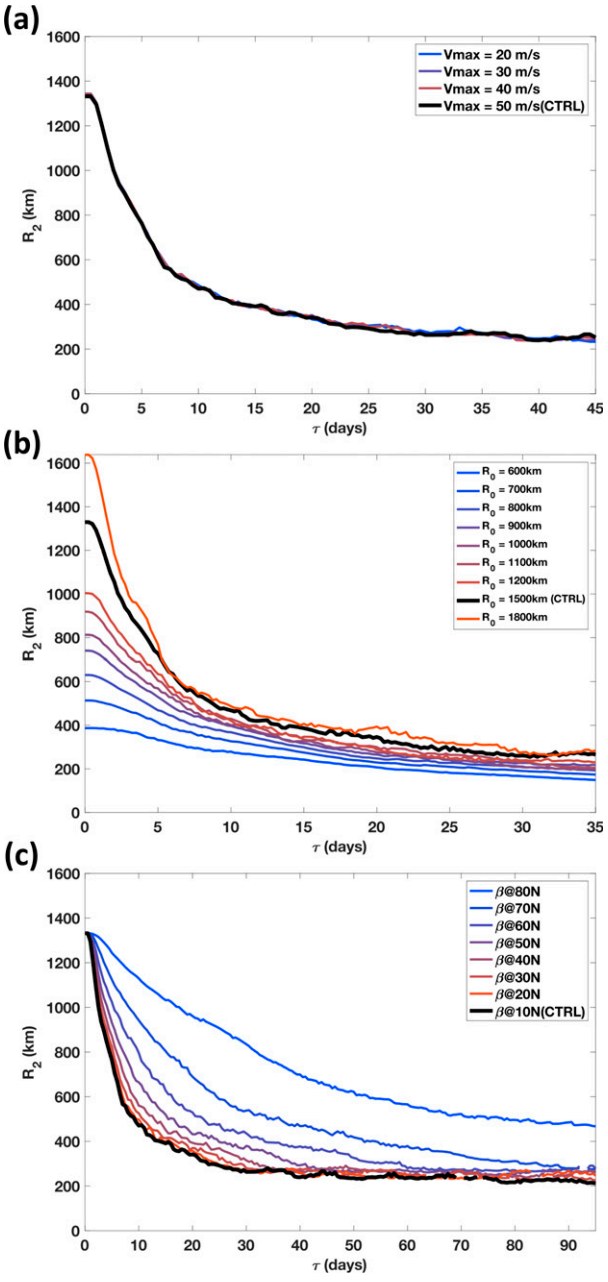

FIG 5. R_2 time series for all three experiment sets: (a) VARYVMAX, (b) VARYR0, and (c) VARYBETA. CTRL is highlighted in thicker black curves across experiment sets.

We begin with VARYR0. Figure 6a shows R_2/R_{VRS_0} for VARYR0. Warmer colors represent members with larger initial R_2/R_{VRS_0}. As mentioned above, each member in VARYR0 has different initial R_2/R_{VRS_0} due principally to the different initial vortex size. Experiments with higher initial R_2/R_{VRS_0} will decrease in size faster, especially for the first 5 days of the experiment, which is a strong evidence in support of our hypothesis. All members' R_2/R_{VRS_0} eventually converge to a value slightly smaller than 1 in the quasi-equilibrium stage, indicating that each vortex shrinks to a size slightly smaller than its initial R_{VRS}. Moreover, all experiments' time series converge to nearly the same curve as they approach the quasi-equilibrium stage, in contrast to the dimensional case (Fig. 5). This result indicates that R_{VRS_0} imposes a strong limit on equilibrium vortex size. Note that, though each experiment starts from a different initial R_2/R_{VRS_0}, they all reach their quasi-equilibrium stage at similar times, indicating that they have different shrinking rates but a similar overall equilibration time scale.

We next propose to nondimensionalize experiment time τ by the initial vortex Rhines time scale T_{VRS_0} [Eq. (8)]. To examine whether T_{VRS_0} can represent the vortex size shrinking time scale across experiments, we nondimensionalize time with the value of T_{VRS_0} to test if the curves will further collapse together. Note that a time-varying T_{VRS} cannot be used here; a single constant time scale must be chosen. Figure 6b shows the evolution of R_2/R_{VRS_0} versus τ/T_{VRS_0} for VARYR0. Doing so produces a similar evolution toward equilibrium across experiments but with the curves seemingly shifted in time. This behavior suggests that the size evolution depends solely on the present value of R_2/R_{VRS_0}, with experiments that begin at a larger value of R_2/R_{VRS_0} taking longer to reach equilibrium. To demonstrate this, as a final step we shift the curves in time to align with the curve with the CTRL (see Fig. 6c). The final result yields curves that approximately collapse to a single universal curve. This outcome confirms that T_{VRS_0} represents the time scale associated with the shrinking rate of each experiment, and that the evolution depends only on the current value of R_2/R_{VRS_0}.

Next we analyze VARYBETA. Figure 6d is the same as Fig. 6a, but for VARYBETA. Each member has different initial R_2/R_{VRS_0} due to the different initial R_{VRS}. Similar to VARYR0, members in VARYBETA with larger initial R_2/R_{VRS_0} also shrink faster and also converge to a value smaller than 1 in the quasi-equilibrium stage. However, in contrast to VARYR0, members in VARYBETA equilibrate over significantly different time scales, especially for members with lower β, indicating that they have different underlying time scales. Thus, we nondimensionalize time in Fig. 6e, which shows R_2/R_{VRS_0} versus τ/T_{VRS_0}. Beyond an initial period of rapid shrinking (i.e., nondimensional time equals to 5 onward), the simulations now collapse well through to equilibrium, such that all members reach equilibrium at the same time. The curves do not collapse closely during the shrinking stage, indicating perhaps some additional dynamics at play that cannot be captured via our two dominant vortex Rhines scale parameters; note that a time translation similar to that done for VARYR0 will not help further collapse these curves since they shrink at different rates.

To understand how T_{VRS_0} varies across experiments, Fig. 7 shows the relation between T_{VRS_0} and the initial R_2/R_{VRS_0} of all members in VARYR0 and VARYBETA. In VARYBETA, a vortex at larger β (lower latitude) at fixed initial R_0 will have a smaller R_{VRS_0} but a larger U_{VRS_0}, which both act to decrease T_{VRS_0} [Eq. (8)]; thus, T_{VRS_0} decreases rapidly as β is increased. On the other hand, in VARYR0, a vortex with a larger initial R_0 at fixed β will have a larger R_{VRS_0} and U_{VRS_0}, whose effects on T_{VRS_0} oppose one another; thus, T_{VRS_0} decreases slowly as

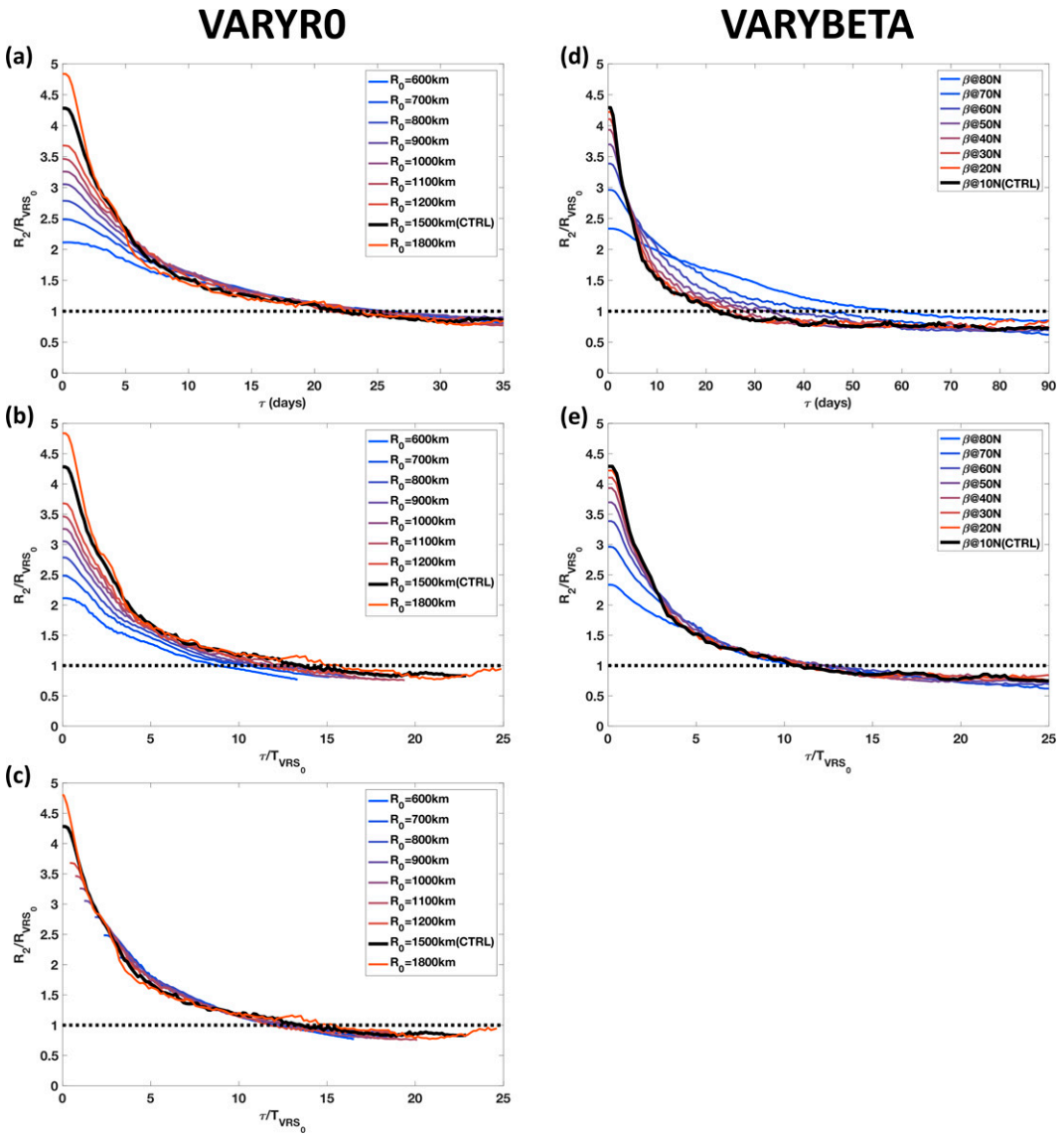

FIG 6. Results from Fig. 5b and 5c for (left) VARYR0 and (right) VARYBETA in nondimensional space. (a) R_2/R_{VRS_0} vs τ for VARYR0. (b) As in (a), but with time nondimensionalized by T_{VRS_0}, τ/T_{VRS_0}. (c) As in (b), but with curves are shifted in time to align with the CTRL. (d) As in (a), but for VARYBETA. (e) As in (b), but for VARYBETA.

R_0 is increased. Thus, the behavior of $T_{VRS,0}$ differs when R_2/R_{VRS} is varied by changing R_0 versus β. Basic physical insight into the meaning of this time scale is provided in section 4g below.

Across both experiment sets, our results show that nondimensionalization of radius and time by R_{VRS_0} and T_{VRS_0}, respectively, can allow all curves to significantly collapse with each other. The broad implication is that R_2 shrinks toward R_{VRS_0} over a fundamental time scale given by T_{VRS_0}, though it occurs in slightly different ways when varying R_0 versus β. For VARYR0, the curves collapse at all times via a time translation, indicating that there is a universal nondimensional shrinking rate that only depends on the current value of R_2/R_{VRS_0} (i.e., the size evolution is path independent), and T_{VRS_0} represents the time scale of this rate. For VARYBETA, each curve is initially different but all curves converge to 1 over a specific single time scale, and T_{VRS_0} represents this overall equilibration time scale. Why this distinction arises between the two experiment types is not currently known but may be related to the wave dynamics in the outer region that differs when varying storm size (R_0 of U_c profile) versus varying β (slope of U_{Rh}).

e. *The evolution of the vortex Rhines scale*

We have demonstrated how we can understand the vortex size evolution using *initial* values of R_{VRS_0} and T_{VRS_0}. We found that knowledge of the initial vortex structure and β

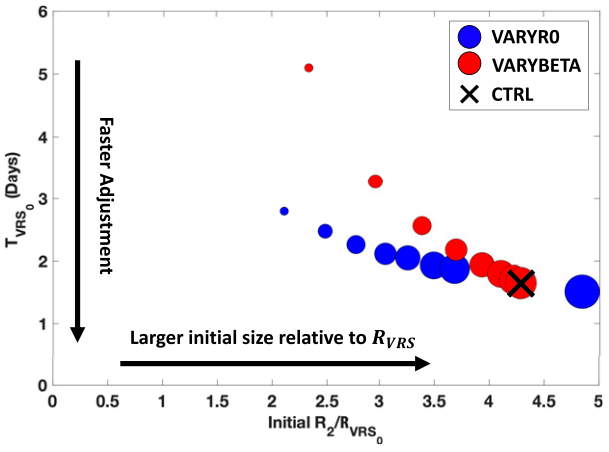

FIG 7. Scatterplot of T_{VRS_0} against initial R_2/R_{VRS_0} for experiment sets VARYR0 and VARYBETA. CTRL is highlighted with a black cross. Larger marker size represents member with larger magnitude R_0 or β within the relevant experiment set.

value alone are sufficient to predict both the upper limit on equilibrium vortex size (R_{VRS_0}) and the shrinking time scale (T_{VRS_0}). However, R_{VRS} may also change with time during a given experiment. We may also use the time-dependent R_{VRS} to normalize R_2 (Figs. 8a,c), which yields very similar results to that presented above using R_{VRS_0}. The only difference is that the R_2/R_{VRS} curves converge to an equilibrium value that is almost exactly 1, rather than a bit smaller than 1 in Fig. 6, indicating that the final equilibrium size is almost exactly given by R_{VRS}. Although normalizing by the time-dependent R_{VRS} is technically more precise, it requires knowledge of the vortex evolution itself and hence is no longer a true prediction.

R_{VRS_0} may be used instead of the time-dependent R_{VRS} because the intrinsic time scale of R_{VRS} relative to its initial value R_{VRS_0} also follows T_{VRS_0}. (Recall that T_{VRS_0} must be used, as a time-varying T_{VRS} does not make sense for our analysis.) The relation between $R_2/\mathrm{R}_{\mathrm{VRS}}$ and R_2/R_{VRS_0} can be written as following:

$$\frac{R_2}{R_{\mathrm{VRS}_0}} = \frac{R_{\mathrm{VRS}}}{R_{\mathrm{VRS}_0}} \frac{R_2}{R_{\mathrm{VRS}}}. \tag{9}$$

Mathematically, if the evolution of R_2/R_{VRS} and $R_{\mathrm{VRS}}/R_{\mathrm{VRS}_0}$ both collapse across experiments after nondimensionalizing by T_{VRS_0}, then R_2/R_{VRS_0} will collapse as well. Figures 8b and 8d show $R_{\mathrm{VRS}}/R_{\mathrm{VRS}_0}$ versus τ/T_{VRS_0} for VARYR0 and VARYBETA, respectively. For both experiment sets, all curves nearly collapse, indicating that R_{VRS} decreases relative to their initial values at the same nondimensional rate. For this reason, R_2/R_{VRS} and R_2/R_{VRS_0} yield similar nondimensional results. Using the initial value is therefore preferable since it is

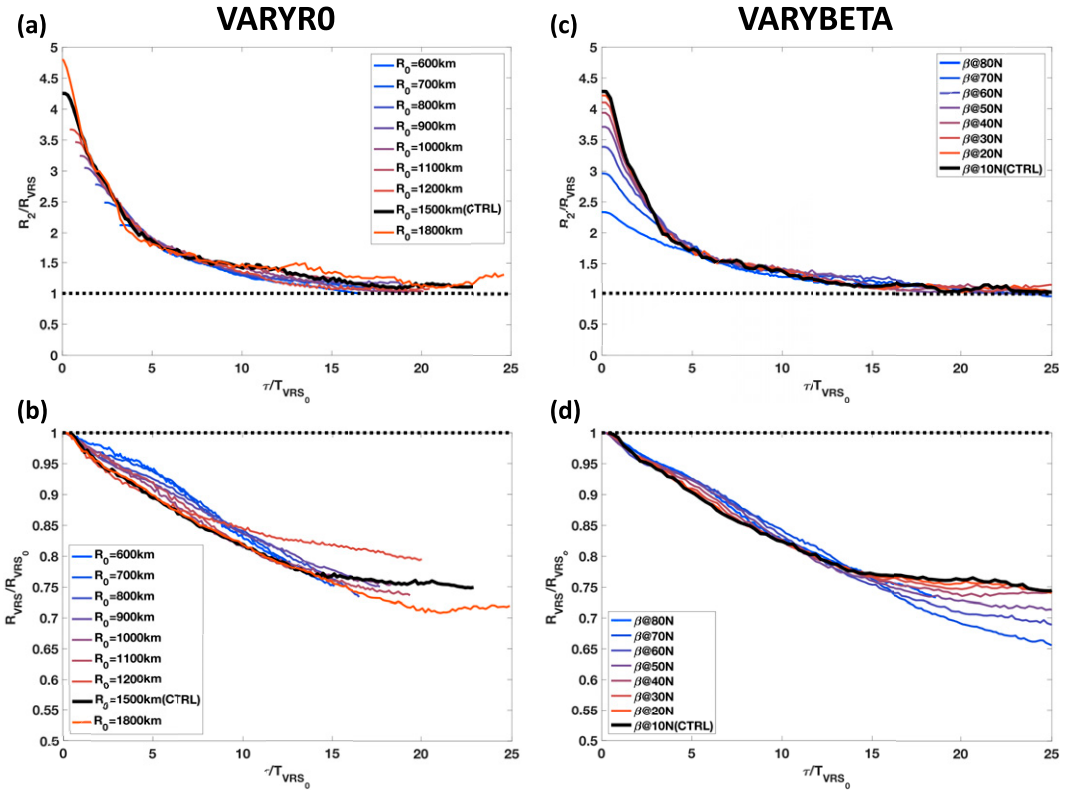

FIG 8. Nondimensional evolution of R_2 relative to R_{VRS}, and R_{VRS} from its initial value R_{VRS_0}. (a) R_2/R_{VRS} vs τ/T_{VRS_0} for VARYR0, and curves are shifted in time to align with the CTRL. (b) $R_{\mathrm{VRS}}/R_{\mathrm{VRS}_0}$ vs τ/T_{VRS_0} for VARYR0. (c) As in (a), but for VARYBETA, and without time translation. (d) As in (b), but for VARYBETA.

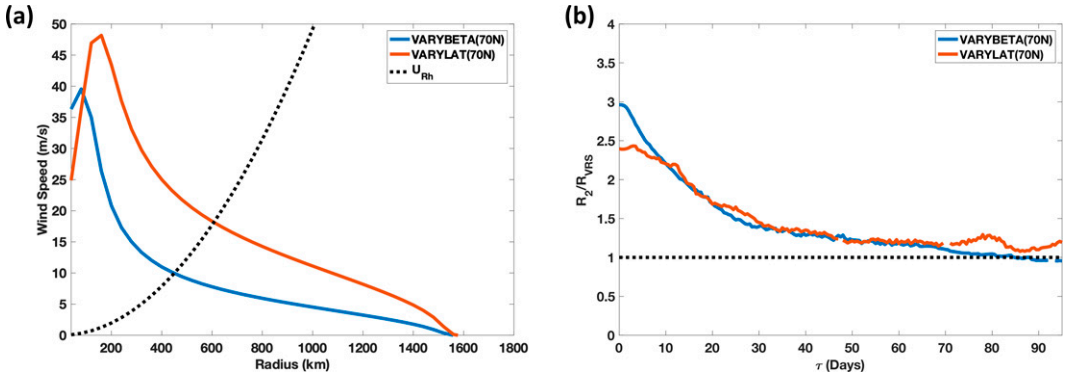

FIG 9. Comparison of 70°N experiment from VARYBETA with VARYLAT(70N). (a) Initial U_c profiles and their U_{Rh} profile (dashed curve). (b) R_2/R_{VRS}.

knowable a priori, and hence, it can be used to predict how vortex size on a β plane will evolve with time. This result further highlights how T_{VRS_0} is the dominant intrinsic time scale for this system.

f. A more Earthlike case: Allowing f to vary

In VARYBETA we only modified the value of β in the barotropic model while leaving f constant when specifying the initial vortex using the C15 model. In the real world on a rotating sphere, changing latitude will change β and f simultaneously. Allowing f to change in the C15 model while holding R_0 fixed will change the radial structure of the resulting wind profile inside of R_0.

Here we briefly test whether changing f consistent with a change in β (i.e., true changes in latitude) on Earth will affect our result significantly. To do so, we perform an experiment identical to our VARYBETA experiment at 70°N except with a vortex generated by the C15 model with f set at its value at 70°N [hereafter VARYLAT(70N)], and compare the results. Figure 9a shows the initial U_c profiles; the U_{Rh} profile is identical for each. Larger f shifts the wind field structure radially outwards toward R_0, including a larger $R_{\max}$ (which results in larger $V_{\max}$ when inserted into the barotropic model) and stronger winds at most radii beyond the inner core.

Figure 9b shows R_2/R_{VRS} between these two experiments. Results show that despite different initial R_2/R_{VRS}, the two members from VARYBETA and VARYLAT(70N) have similar R_2/R_{VRS} evolution after 10 days. This indicates that our overall results are not dependent on holding f fixed in the wind profile and hence may be directly applicable to the real Earth.

g. Linking T_{VRS} to the Rossby wave group velocity

The dynamical details of the vortex–wave interaction, in particular a mechanistic understanding of the waves themselves and the energy transfer that they induce, are not tackled in this work. Here, though, we provide a simple first step in this direction by linking T_{VRS} to the Rossby wave group velocity. We defined T_{VRS} as the overturning time scale of the circulation at R_{VRS}, which can be written as a function of R_{VRS} and β:

$$T_{\mathrm{VRS}} = \frac{2\pi R_{\mathrm{VRS}}}{U_{\mathrm{VRS}}} = \frac{2\pi R_{\mathrm{VRS}}}{2\pi\beta {R_{\mathrm{VRS}}}^2} = \frac{1}{\beta R_{\mathrm{VRS}}}, \tag{10}$$

where we have made use of the fact that the U_{VRS} can be defined using the definition of the Rhines speed [Eq. (5)] as $U_{\mathrm{Rh}}(r = R_{\mathrm{VRS}})$. Following the theory discussed above, at R_{VRS} the circulation's overturning time scale should equal the planetary Rossby wave generation time scale, which we propose should be directly related to the time scale of planetary Rossby wave propagation T_{RW}. Here, similar to how we calculate T_{VRS}, we estimate the T_{RW} by using the circulation's circumference as the length scale, and the group velocity of the planetary Rossby wave ($c_{g\mathrm{RW}}$) as its propagation speed:

$$T_{\mathrm{RW}} \propto \frac{2\pi R_{\mathrm{VRS}}}{c_{g\mathrm{RW}}}. \tag{11}$$

For a barotropic planetary Rossby wave, its group velocity is given by (Vallis 2017, p. 228):

$$c_{g\mathrm{RW}} = \sqrt{c_g^{x2} + c_g^{y2}} = \sqrt{\left[\frac{\beta(k^2 - l^2)}{(k^2 + l^2)^2}\right]^2 + \left[\frac{2kl\beta}{(k^2 + l^2)^2}\right]^2}, \tag{12}$$

where k and l are the wavenumbers in the x and y direction, respectively, and c_g^x and c_g^y are the Rossby wave group velocity in the x and y direction, respectively. For a vortex we assume axisymmetry, such that $k = l$, which results in zero group velocity in the x direction. We take wavenumber to be inversely proportional to the circulation's circumference [$k \approx 1/(2\pi R_{\mathrm{VRS}})$]. The group velocity at R_{VRS} may then be written as

$$c_{g\mathrm{RW}} = c_g^y = \frac{2kl\beta}{(k^2 + l^2)^2} = \frac{2k^2\beta}{(k^2 + k^2)^2} = \frac{\beta}{2k^2} \approx 2\beta\pi^2 R_{\mathrm{VRS}}^2. \tag{13}$$

And now we can substitute Eq. (13) into Eq. (11) to write T_{RW} in terms of R_{VRS}:

$$T_{\mathrm{RW}} \propto \frac{2\pi R_{\mathrm{VRS}}}{2\beta\pi^2 R_{\mathrm{VRS}}^2} = \frac{1}{\pi\beta R_{\mathrm{VRS}}}. \quad (14)$$

Comparing Eq. (14) to Eq. (10), we find that T_{RW} is identical in form to T_{VRS}, differing only by a factor π. The similarity between T_{RW} and T_{VRS} indicates that T_{VRS} is proportional to the planetary Rossby wave propagation time scale at R_{VRS}, which should be directly related to the wave-induced dissipation of the vortex outer circulation that drives the size evolution of a TC-like vortex on a β plane. This basic theoretical linkage, in conjunction with our results and conceptual understanding above, provides further insight into how the vortex Rhines scale governs the first-order dynamics of the vortex response to β. Understanding the detailed radial structure of these waves may provide deeper insight and is left for future work.

5. Conclusions and discussion

a. Summary

This study derives a new concept called the vortex Rhines scale and applies it to experiments with a nondivergent 2D barotropic model to understand how β limits the size of a tropical cyclone–like vortex. Since the nondivergent barotropic vorticity equation includes only the advection of the relative and planetary vorticity, our experiment design provides an idealized and straightforward framework to investigate the dynamics of a TC-like vortex in the presence of β and its relationship to the traditional Rhines scale. The key findings of this study are as follows:

1) We derive a quantity called the vortex Rhines scale (R_{VRS}), which translates the traditional Rhines scale into the context of an individual axisymmetric vortex, and show how it can be used to understand the effect of β on a TC-like vortex.
2) The vortex Rhines scale serves as a robust limit on the size of a TC-like vortex on a barotropic β plane, which corroborates the finding in CR19 that storm size scales with the traditional Rhines scale. The circulation beyond the vortex Rhines scale will weaken with time, which manifests itself as a shrinking of vortex size. R_{VRS} offers a more useful scale for the limit of TC size than the traditional Rhines scale.
3) Theoretically, the vortex will be divided into two regions by R_{VRS}: the vortex region at smaller radii and the wave region at larger radii. In the vortex region, the circulation is highly axisymmetric and largely unaffected by β. In the wave region, planetary Rossby wave generation is strong, and waves distort and dissipate the outer circulation.
4) A larger vortex relative to its R_{VRS} will shrink faster, and all vortices shrink toward an equilibrium close to its vortex Rhines scale.
5) Vortex size shrinks toward R_{VRS} following a dominant time scale given by T_{VRS}, though the role of that time scale differs slightly when varying R_0 versus β. T_{VRS} is also shown to be closely related to the Rossby wave group velocity at the vortex Rhines scale, which provides a direct link between our theory and the dynamics of the waves themselves.
6) The first-order evolution of the vortex for any value of R_0 and β is controlled by the initial value of R_{VRS} and T_{VRS}, thereby enabling one to predict the vortex response from the initial condition alone.
7) A similar outcome occurs when allowing f in the initial vortex structure to change consistent with β, indicating that the results are also applicable to an Earthlike setting.

b. Relevance to TCs on Earth

It is important to place our idealized results in the context of real TCs on Earth. The typical duration of a TC is on the order of 10 days (Webster et al. 2005) and form from preexisting disturbances that may have propagated for much longer. Since most of our experiment members (especially for those on a lower latitude β plane) have shrunk rapidly within 10 days, the vortex Rhines scale would be expected to strongly limit TC size on Earth. Moreover, it explains how storm size may vary widely in nature, as TC size may remain steady at any size that is reasonably small relative to this scale, since the vortex Rhines scale only sets an upper bound on vortex size. Additionally, R_{VRS} in our experiments range from 200 to 400 km, which is substantially smaller than the f^{-1} theoretical length scale for TC size on the f plane, V_p/f, where V_p is the potential intensity (Chavas and Emanuel 2014), which is larger than 1000 km at low latitudes (and goes to infinity at the equator). In other words, if a TC were to form with a size equal to V_p/f, our results indicate that β and its induced wave effects would cause it to shrink rapidly within a few days. This is a simple mechanistic explanation for why V_p/f is not an appropriate scaling for TC size in the tropics, confirming the conclusion found in observations (Chavas et al. 2016). Instead, TCs at low latitudes should feel R_{VRS} strongly. Since β decreases slowly with latitude in the tropics, R_{VRS} should increase slowly with latitude. This variation is consistent with the gradual increase in storm size with latitude seen in observations and in aquaplanet experiments in CR19. Note that our β-plane model does not have f at all, so it cannot be used to test the V_p/f scaling nor its role relative to R_{VRS} in tropical region. Future work can test this with a more complex model.

In all of our experiments, when initializing the barotropic model with a TC-like vortex from C15 model, all vortices will shrink in size after turning on β. This does not suggest that the size of initial wind profile from C15 model can never be reached on a β plane, and our results do not reject the C15 model. The reason why all profiles from the C15 model shrink in our experiments is because there are no other processes that can maintain the outer circulation in the barotropic model, only the effect of the β term exists and it acts to shrink the vortex. The solution for the outer circulation wind field in the C15 model is derived from the assumption that Ekman suction associated with radial inflow matches free-tropospheric radiative cooling due to the mass continuity (Chavas et al. 2015). Neither of these processes are permitted in our barotropic model. Thus, we initialize the model with a realistic wind profile based on C15 model solution for an

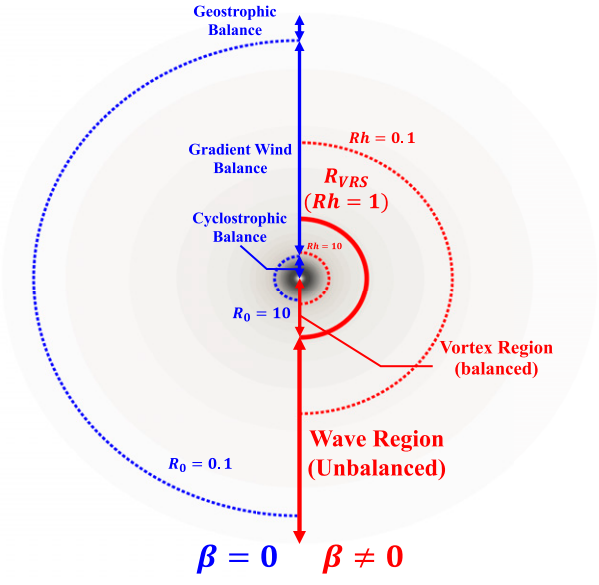

FIG 10. Conceptual diagram illustrating the different dynamical regimes associated with f (left half) and β (right half) in a vortex. Blue dotted circles represent the radius of different values of the Rossby number, and blue arrows indicate key dynamical balance regimes associated with f. Red dotted circles represent the radius of different values of the Rhines number, and R_{VRS} (where Rh = 1) is highlighted by a thicker solid red circle. Red arrows indicate the quasi-balanced vortex region and unbalanced wave region. Wind field is the CTRL vortex of Fig. 3.

equilibrium structure, but then this structure is free to evolve away from that solution since the C15 physics are not included in the barotropic model.

c. Other considerations

Commonly used definitions of TC size typically describe some aspect of the TC structure and the horizontal distribution of some properties, such as the radius of a fixed wind speed. In contrast, R_{VRS} defines a specific boundary between two different dynamical regions (vortex region and wave region). Hence, R_{VRS} represents a size toward which a storm may shrink from its present size.

Though our derivations and analyses have assumed axisymmetry, these physics may be general to any vortex, even asymmetric ones such as extratropical cyclones. Indeed, our results and theory suggests a simple mechanistic explanation for why the Rhines scale cuts of the upscale energy cascade in 2D turbulence and limits extratropical cyclone size (e.g., Held and Larichev 1996; Chai and Vallis 2014; Chemke and Kaspi 2015, 2016; Chemke et al. 2016). We arrive at a similar conclusion by considering a single coherent and well-defined eddy, rather than the statistics of eddies in an equilibrated turbulent flow.

The essence of the Rhines effect on a vortex is the interaction between the vortex and the planetary Rossby waves stimulated by the circulation of the vortex at relatively large radii. Though we have used T_{VRS} to show the relationship between the vortex Rhines scale and Rossby wave group velocity, wave activity is not directly diagnosed in this study. Detailed analysis of the dynamics of wave activity within our experiment setup may be a fruitful avenue for future work.

All of our experiments are on a single 2D nondivergent barotropic model. This simplified approach omits various key physical features in real TCs, but it is unclear how nonbarotropic effects would modify these barotropic responses. Further investigation in models with higher degrees of complexity and in observations is needed to evaluate our findings in a full-physics baroclinic environment.

d. Relationship to Rossby number and common dynamical balance regimes

Finally, to provide a broader perspective on our findings, we conclude with a simple conceptual diagram to place the effect of β in the context of standard dynamical balance regimes common in atmospheric science. Figure 10 shows the 2D TC wind field of the CTRL vortex with radii highlighted where the Rossby number (Ro) and Rhines number (Rh) each cross order-of-magnitude thresholds. In the presence of f, the Rossby number (blue dotted circles) is used to define balanced flow regimes. Within the inner core region (inside of Ro = 10 circle in Fig. 10), Ro is significantly larger than 10, which corresponds to cyclostrophic balance. Between the inner core and far outer circulation, Ro ranges between 0.1 and 10, which corresponds to gradient wind balance. Finally, in the far outer circulation inside of the outer radius, Ro is less than 0.1, which corresponds to geostrophic balance. In the presence of β (Fig. 10, right half), the Rhines effect introduces an unbalanced regime at radii beyond the vortex Rhines scale (Rh $<$ 1) where planetary Rossby waves are readily generated by the vortex flow that gradually weakens the flow. Note that the region of 10 $>$ Rh $>$ 0.1 is relatively narrow due to a faster increase in Rh with radius. The strong radial gradient of Rh further indicates that the vortex Rhines scale can strongly limit vortex size.

Acknowledgments. The authors thank Dr. Malte Jansen for suggesting testing the vortex Rhines time scale. Data and scripts for all figures in this paper are available on PURR: https://purr.purdue.edu/publications/4027/1. Funding support was provided by NSF Grants 1826161 and 1945113. Computing resources for this work were generously supported by Purdue's Rosen Center for Advanced Computing and the Community Cluster Program (McCartney et al. 2014).

REFERENCES

Chai, J., and G. K. Vallis, 2014: The role of criticality on the horizontal and vertical scales of extratropical eddies in a dry GCM. *J. Atmos. Sci.*, **71**, 2300–2318, https://doi.org/10.1175/JAS-D-13-0351.1.

Chan, J. C. L., and R. T. Williams, 1987: Analytical and numerical studies of the beta-effect in tropical cyclone motion. Part I: Zero mean flow. *J. Atmos. Sci.*, **44**, 1257–1265, https://doi.org/10.1175/1520-0469(1987)044<1257:AANSOT>2.0.CO;2.

Chan, K. T. F., and J. C. L. Chan, 2013: Angular momentum transports and synoptic flow patterns associated with tropical

cyclone size change. *Mon. Wea. Rev.*, **141**, 3985–4007, https://doi.org/10.1175/MWR-D-12-00204.1.

Chavas, D. R., 2022: Code for tropical cyclone wind profile model of Chavas et al (2015, JAS). Purdue University Research Repository, https://doi.org/10.4231/CZ4P-D448.

——, and K. Emanuel, 2014: Equilibrium tropical cyclone size in an idealized state of axisymmetric radiative–convective equilibrium. *J. Atmos. Sci.*, **71**, 1663–1680, https://doi.org/10.1175/JAS-D-13-0155.1.

——, and N. Lin, 2016: A model for the complete radial structure of the tropical cyclone wind field. Part II: Wind field variability. *J. Atmos. Sci.*, **73**, 3093–3113, https://doi.org/10.1175/JAS-D-15-0185.1.

——, and K. A. Reed, 2019: Dynamical aquaplanet experiments with uniform thermal forcing: System dynamics and implications for tropical cyclone genesis and size. *J. Atmos. Sci.*, **76**, 2257–2274, https://doi.org/10.1175/JAS-D-19-0001.1.

——, N. Lin, and K. Emanuel, 2015: A model for the complete radial structure of the tropical cyclone wind field. Part I: Comparison with observed structure. *J. Atmos. Sci.*, **72**, 3647–3662, https://doi.org/10.1175/JAS-D-15-0014.1.

——, ——, W. Dong, and Y. Lin, 2016: Observed tropical cyclone size revisited. *J. Climate*, **29**, 2923–2939, https://doi.org/10.1175/JCLI-D-15-0731.1.

Chemke, R., and Y. Kaspi, 2015: The latitudinal dependence of atmospheric jet scales and macroturbulent energy cascades. *J. Atmos. Sci.*, **72**, 3891–3907, https://doi.org/10.1175/JAS-D-15-0007.1.

——, and ——, 2016: The latitudinal dependence of the oceanic barotropic eddy kinetic energy and macroturbulence energy transport. *Geophys. Res. Lett.*, **43**, 2723–2731, https://doi.org/10.1002/2016GL067847.

——, T. Dror, and Y. Kaspi, 2016: Barotropic kinetic energy and enstrophy transfers in the atmosphere. *Geophys. Res. Lett.*, **43**, 7725–7734, https://doi.org/10.1002/2016GL070350.

DeMaria, M., 1985: Tropical cyclone motion in a nondivergent barotropic model. *Mon. Wea. Rev.*, **113**, 1199–1210, https://doi.org/10.1175/1520-0493(1985)113<1199:TCMIAN>2.0.CO;2.

Dunion, J. P., C. D. Thorncroft, and C. S. Velden, 2014: The tropical cyclone diurnal cycle of mature hurricanes. *Mon. Wea. Rev.*, **142**, 3900–3919, https://doi.org/10.1175/MWR-D-13-00191.1.

Eames, I., and J.-B. Flór, 2002: The dynamics of monopolar vortices on a topographic beta plane. *J. Fluid Mech.*, **456**, 353–376, https://doi.org/10.1017/S0022112001007728.

Emanuel, K., 2004: Tropical cyclone energetics and structure. *Atmospheric Turbulence and Mesoscale Meteorology*, Vol. 8, Cambridge University Press, 165–191.

——, and R. Rotunno, 2011: Self-stratification of tropical cyclone outflow. Part I: Implications for storm structure. *J. Atmos. Sci.*, **68**, 2236–2249, https://doi.org/10.1175/JAS-D-10-05024.1.

Fiorino, M., and R. L. Elsberry, 1989: Some aspects of vortex structure related to tropical cyclone motion. *J. Atmos. Sci.*, **46**, 975–990, https://doi.org/10.1175/1520-0469(1989)046<0975:SAOVSR>2.0.CO;2.

Flierl, G. R., and K. Haines, 1994: The decay of modons due to Rossby wave radiation. *Phys. Fluids*, **6**, 3487–3497, https://doi.org/10.1063/1.868405.

Frank, W. M., 1977: The structure and energetics of the tropical cyclone I. Storm structure. *Mon. Wea. Rev.*, **105**, 1119–1135, https://doi.org/10.1175/1520-0493(1977)105<1119:TSAEOT>2.0.CO;2.

Frierson, D. M. W., I. M. Held, and P. Zurita-Gotor, 2006: A gray-radiation aquaplanet moist GCM. Part I: Static stability and eddy scale. *J. Atmos. Sci.*, **63**, 2548–2566, https://doi.org/10.1175/JAS3753.1.

Held, I. M., 1999: Planetary waves and their interaction with smaller scales. *The Life Cycles of Extratropical Cyclones*, Amer. Meteor. Soc., 101–109, https://doi.org/10.1007/978-1-935704-09-6_11.

——, and V. D. Larichev, 1996: A scaling theory for horizontally homogeneous, baroclinically unstable flow on a beta plane. *J. Atmos. Sci.*, **53**, 946–952, https://doi.org/10.1175/1520-0469(1996)053<0946:ASTFHH>2.0.CO;2.

Hill, K. A., and G. M. Lackmann, 2009: Influence of environmental humidity on tropical cyclone size. *Mon. Wea. Rev.*, **137**, 3294–3315, https://doi.org/10.1175/2009MWR2679.1.

Hsieh, T.-L., G. A. Vecchi, W. Yang, I. M. Held, and S. T. Garner, 2020: Large-scale control on the frequency of tropical cyclones and seeds: A consistent relationship across a hierarchy of global atmospheric models. *Climate Dyn.*, **55**, 3177–3196, https://doi.org/10.1007/s00382-020-05446-5.

Irish, J. L., D. T. Resio, and D. Divoky, 2011: Statistical properties of hurricane surge along a coast. *J. Geophys. Res.*, **116**, C10007, https://doi.org/10.1029/2010JC006626.

James, I. N., and L. J. Gray, 1986: Concerning the effect of surface drag on the circulation of a baroclinic planetary atmosphere. *Quart. J. Roy. Meteor. Soc.*, **112**, 1231–1250, https://doi.org/10.1002/qj.49711247417.

Khairoutdinov, M., and K. Emanuel, 2013: Rotating radiative-convective equilibrium simulated by a cloud-resolving model. *J. Adv. Model. Earth Syst.*, **5**, 816–825, https://doi.org/10.1002/2013MS000253.

Kidder, S. Q., J. A. Knaff, S. J. Kusselson, M. Turk, R. R. Ferraro, and R. J. Kuligowski, 2005: The tropical rainfall potential (trap) technique. Part I: Description and examples. *Wea. Forecasting*, **20**, 456–464, https://doi.org/10.1175/WAF860.1.

Kidston, J., S. M. Dean, J. A. Renwick, and G. K. Vallis, 2010: A robust increase in the eddy length scale in the simulation of future climates. *Geophys. Res. Lett.*, **37**, L03806, https://doi.org/10.1029/2009GL041615.

Knaff, J. A., S. P. Longmore, and D. A. Molenar, 2014: An objective satellite-based tropical cyclone size climatology. *J. Climate*, **27**, 455–476, https://doi.org/10.1175/JCLI-D-13-00096.1.

Kossin, J. P., J. A. Knaff, H. I. Berger, D. C. Herndon, T. A. Cram, C. S. Velden, R. J. Murnane, and J. D. Hawkins, 2007: Estimating hurricane wind structure in the absence of aircraft reconnaissance. *Wea. Forecasting*, **22**, 89–101, https://doi.org/10.1175/WAF985.1.

Krouse, K. D., A. H. Sobel, and L. M. Polvani, 2008: On the wavelength of the Rossby waves radiated by tropical cyclones. *J. Atmos. Sci.*, **65**, 644–654, https://doi.org/10.1175/2007JAS2402.1.

LaCasce, J. H., and J. Pedlosky, 2004: The instability of Rossby basin modes and the oceanic eddy field. *J. Phys. Oceanogr.*, **34**, 2027–2041, https://doi.org/10.1175/1520-0485(2004)034<2027:TIORBM>2.0.CO;2.

Lam, J. S.-L., and D. G. Dritschel, 2001: On the beta-drift of an initially circular vortex patch. *J. Fluid Mech.*, **436**, 107–129, https://doi.org/10.1017/S0022112001003974.

Lapeyre, G., and I. M. Held, 2003: Diffusivity, kinetic energy dissipation, and closure theories for the poleward eddy heat flux. *J. Atmos. Sci.*, **60**, 2907–2916, https://doi.org/10.1175/1520-0469(2003)060<2907:DKEDAC>2.0.CO;2.

Lavender, S. L., and J. L. McBride, 2021: Global climatology of rainfall rates and lifetime accumulated rainfall in tropical cyclones: Influence of cyclone basin, cyclone intensity and

cyclone size. *Int. J. Climatol.*, **41**, E1217–E1235, https://doi.org/10.1002/joc.6763.

Llewellyn Smith, S. G. L., 1997: The motion of a non-isolated vortex on the beta-plane. *J. Fluid Mech.*, **346**, 149–179, https://doi.org/10.1017/S0022112097006290.

McCartney, G., T. Hacker, and B. Yang, 2014: Empowering faculty: A campus cyberinfrastructure strategy for research communities. *Educause Review*, https://er.educause.edu/articles/2014/7/empowering-faculty-a-campus-cyberinfrastructure-strategy-for-research-communities.

McDonald, N. R., 1998: The decay of cyclonic eddies by Rossby wave radiation. *J. Fluid Mech.*, **361**, 237–252, https://doi.org/10.1017/S0022112098008696.

Merrill, R. T., 1984: A comparison of large and small tropical cyclones. *Mon. Wea. Rev.*, **112**, 1408–1418, https://doi.org/10.1175/1520-0493(1984)112<1408:ACOLAS>2.0.CO;2.

Montgomery, M. T., and R. J. Kallenbach, 1997: A theory for vortex Rossby-waves and its application to spiral bands and intensity changes in hurricanes. *Quart. J. Roy. Meteor. Soc.*, **123**, 435–465, https://doi.org/10.1002/qj.49712353810.

Powell, M. D., and T. A. Reinhold, 2007: Tropical cyclone destructive potential by integrated kinetic energy. *Bull. Amer. Meteor. Soc.*, **88**, 513–526, https://doi.org/10.1175/BAMS-88-4-513.

Rhines, P. B., 1975: Waves and turbulence on a beta-plane. *J. Fluid Mech.*, **69**, 417–443, https://doi.org/10.1017/S0022112075001504.

Rotunno, R., and G. H. Bryan, 2012: Effects of parameterized diffusion on simulated hurricanes. *J. Atmos. Sci.*, **69**, 2284–2299, https://doi.org/10.1175/JAS-D-11-0204.1.

Sanders, F., and R. W. Burpee, 1968: Experiments in barotropic hurricane track forecasting. *J. Appl. Meteor. Climatol.*, **7**, 313–323, https://doi.org/10.1175/1520-0450(1968)007<0313:EIBHTF>2.0.CO;2.

Schenkel, B. A., and R. E. Hart, 2015: An examination of the thermodynamic impacts of western North Pacific tropical cyclones on their tropical tropospheric environment. *J. Climate*, **28**, 7529–7560, https://doi.org/10.1175/JCLI-D-14-00780.1.

Schneider, T., 2004: The tropopause and the thermal stratification in the extratropics of a dry atmosphere. *J. Atmos. Sci.*, **61**, 1317–1340, https://doi.org/10.1175/1520-0469(2004)061<1317:TTATTS>2.0.CO;2.

Smith, K. S., G. Boccaletti, C. C. Henning, I. Marinov, C. Y. Tam, I. M. Held, and G. K. Vallis, 2002: Turbulent diffusion in the geostrophic inverse cascade. *J. Fluid Mech.*, **469**, 13–48, https://doi.org/10.1017/S0022112002001763.

Smith, R. K., H. C. Weber, and A. Kraus, 1995: On the symmetric circulation of a moving hurricane. *Quart. J. Roy. Meteor. Soc.*, **121**, 945–952, https://doi.org/10.1002/qj.49712152412.

Sukoriansky, S., B. Galperin, and V. Perov, 2006: A quasi-normal scale elimination model of turbulence and its application to stably stratified flows. *Nonlinear Processes Geophys.*, **13**, 9–22, https://doi.org/10.5194/npg-13-9-2006.

Sutyrin, G. G., and G. R. Flierl, 1994: Intense vortex motion on the beta plane: Development of the beta gyres. *J. Atmos. Sci.*, **51**, 773–790, https://doi.org/10.1175/1520-0469(1994)051<0773:IVMOTB>2.0.CO;2.

——, J. S. Hesthaven, J. P. Lynov, and J. J. Rasmussen, 1994: Dynamical properties of vortical structures on the beta-plane. *J. Fluid Mech.*, **268**, 103–131, https://doi.org/10.1017/S002211209400128X.

Vallis, G. K., 2017: *Atmospheric and Oceanic Fluid Dynamics*. Cambridge University Press, 773 pp.

——, and M. E. Maltrud, 1993: Generation of mean flows and jets on a beta plane and over topography. *J. Phys. Oceanogr.*, **23**, 1346–1362, https://doi.org/10.1175/1520-0485(1993)023<1346:GOMFAJ>2.0.CO;2.

Wang, B., X. Li, and L. Wu, 1997: Direction of hurricane beta drift in horizontally sheared flows. *J. Atmos. Sci.*, **54**, 1462–1471, https://doi.org/10.1175/1520-0469(1997)054<1462:DOHBDI>2.0.CO;2.

Weatherford, C. L., and W. M. Gray, 1988a: Typhoon structure as revealed by aircraft reconnaissance. Part I: Data analysis and climatology. *Mon. Wea. Rev.*, **116**, 1032–1043, https://doi.org/10.1175/1520-0493(1988)116<1032:TSARBA>2.0.CO;2.

——, and ——, 1988b: Typhoon structure as revealed by aircraft reconnaissance. Part II: Structural variability. *Mon. Wea. Rev.*, **116**, 1044–1056, https://doi.org/10.1175/1520-0493(1988)116<1044:TSARBA>2.0.CO;2.

Webster, P. J., G. J. Holland, J. A. Curry, and H.-R. Chang, 2005: Changes in tropical cyclone number, duration, and intensity in a warming environment. *Science*, **309**, 1844–1846, https://doi.org/10.1126/science.1116448.

Wu, L., W. Tian, Q. Liu, J. Cao, and J. A. Knaff, 2015: Implications of the observed relationship between tropical cyclone size and intensity over the western North Pacific. *J. Climate*, **28**, 9501–9506, https://doi.org/10.1175/JCLI-D-15-0628.1.

Zhou, W., I. M. Held, and S. T. Garner, 2014: Parameter study of tropical cyclones in rotating radiative–convective equilibrium with column physics and resolution of a 25-km GCM. *J. Atmos. Sci.*, **71**, 1058–1069, https://doi.org/10.1175/JAS-D-13-0190.1.